Parameterization of Vertical Mixing in Numerical Models of Tropical Oceans

R. C. PACANOWSKI AND S. G. H. PHILANDER

Geophysical Fluid Dynamics Laboratory/NOAA, Princeton University, Princeton, NJ 08540

(Manuscript received 28 January 1981, in final form 18 August 1981)

ABSTRACT

Measurements indicate that mixing processes are intense in the surface layers of the ocean but weak below the thermocline, except for the region below the core of the Equatorial Undercurrent where vertical temperature gradients are small and the shear is large. Parameterization of these mixing processes by means of coefficients of eddy mixing that are Richardson-number dependent, leads to realistic simulations of the response of the equatorial oceans to different windstress patterns. In the case of eastward winds results agree well with measurements in the Indian Ocean. In the case of westward winds it is of paramount importance that the nonzero heat flux into the ocean be taken into account. This heat flux stabilizes the upper layers and reduces the intensity of the mixing, especially in the east. With an appropriate surface boundary condition, the results are relatively insensitive to values assigned to constants in the parameterization formula.

1. Introduction

Mixing processes are of great importance near the ocean surface. Kraus and Turner (1967) parameterized this mixing in a model that takes into account the effects of wind-stirring, and of entrainment across the lower boundary of the mixed layer. Since the model neglects the dynamical response of the ocean to variable winds it is successful in regions where mixed-layer properties are determined primarily by the local fluxes (of heat and momentum) across the ocean surface. The model fails in the tropics where the effect of these local fluxes can be secondary to effects associated with a horizontal redistribution of heat in the upper ocean. This happens when the response of the ocean to changing surface winds includes a change in the topography of the thermocline. In Fig. 1a for example, the pronounced zonal slope of isotherms in the equatorial plane is caused by the westward surface winds (which accumulate warm water in the west and expose cold water in the east). A relaxation of the winds will cause the thermocline to become horizontal. In the process, a large amount of heat is transferred from west to east. The mixed layer in the eastern equatorial Pacific therefore changes enormously even though local fluxes across the ocean surface may not change. The point is that, in the upper layers of the tropical oceans, both fluxes across the surface, and the dynamical response to variable winds are important, even on time-scales as short as a month.

Hughes (1980) recently developed an equatorial mixed-layer model that includes the effects of wind-stirring and entrainment according to the Kraus-Turner formulation. The model also takes some aspects of the dynamical response of the ocean into account but it is unfortunately too simple to cope with the horizontal redistribution of heat (mentioned earlier) that is believed to be of paramount importance in the tropics.

Multilevel numerical models that are capable of simulating the dynamical response of the ocean usually parameterize mixing processes in a very crude manner because constant values are assigned to the mixing parameters, namely, the coefficients of vertical eddy viscosity ν and eddy diffusivity κ. Measurements show that these parameters vary considerably in the tropical oceans. They usually have large values in the mixed surface layer, but have very small values below the thermocline. Halpern (1980), for example, finds that the value for ν varies from 30 to 100 cm^2 s^{-1} in the mixed layer near 8°N, 23°W (which is in the North Equatorial Countercurrent in the Atlantic Ocean). The value for ν in and below the thermocline, however, is substantially smaller. In the region of the Equatorial Undercurrent mixing processes can be intense both above and below the thermocline presumably because of the large vertical shears associated with the current. Below the core of the Undercurrent there is sufficient mixing to give rise to a thermostad —a region with very small vertical density gradients and an average temperature of 13°C. The measurements of Crawford and Osborn (1979a,b) suggest that in this thermostad ν has a value that varies approximately from 2 to 11 cm^2 s^{-1}. At the core of the Undercurrent the value is of order 1 cm^2 s^{-1} and

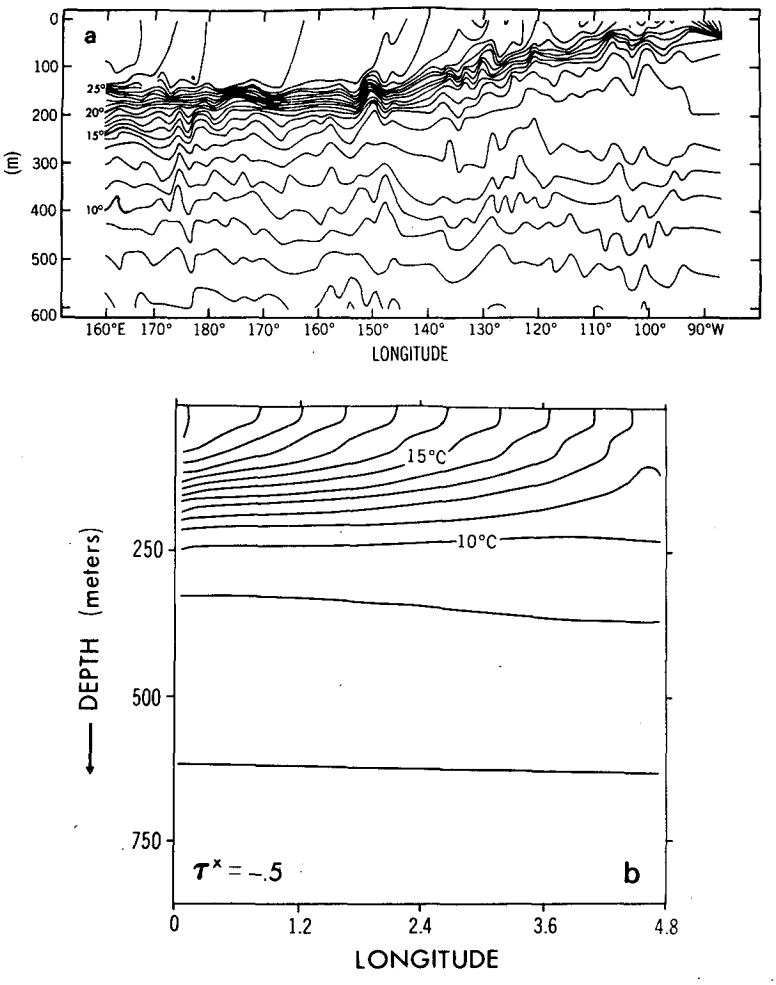

FIG. 1. Temperature as a function of depth and longitude along the equator (a) as observed in the Pacific Ocean by Colin *et al.* (1971) and (b) as simulated with the model of *PP* in which ν and κ have constant values. (Longitude is measured in units of 1000 km.)

above the core it varies from 8 to 100 cm^2 s^{-1}. Jones (1973) and Gregg (1976) obtain similar results from the Pacific Ocean. (see also Katz *et al.*, 1979).

If the results from numerical models were insensitive to the constant values assigned to ν and κ then there would be no need for concern. But this is not the case. Philander and Pacanowski (1980), hereafter referred to as *PP*, find that the maximum speed of the Equatorial Undercurrent in their model increases from 50 to 75 cm s^{-1} when the value of ν is decreased from 10 to 5 cm^2 s^{-1}. In the model of Semtner and Holland (1980), the Undercurrent attains speeds of 100 cm s^{-1} in the time average. The principal reason for this may be the small value for v in that model.

In this paper we explore non-constant parameterizations for ν and κ. The measurements of Crawford and Osborn (1979a) and Osborn and Bilodean (1980) suggest that mixing processes are strongly influenced by the shears of the mean currents. Empirical studies (see Robinson 1966; Jones, 1973) indicate that the shear dependence of ν and κ should be of the following form:

$$\nu = \frac{\nu_0}{(1 + \alpha\ \mathrm{Ri})^n} + \nu_b, \tag{1}$$

$$\kappa = \frac{\nu}{(1 + \alpha\ \mathrm{Ri})} + \kappa_b, \tag{2}$$

where the Richardson number

$$\mathrm{Ri} = \frac{\beta g T_z}{U_z^2 + V_z^2} \tag{3}$$

and the coefficient of thermal expansion of water

$$\beta \sim 8.75 \times 10^{-6}(T + 9).$$

Here T denotes the potential temperature in °C, U and V are the horizontal velocity components, g is the gravitational acceleration, ν_b and κ_b are background dissipation parameters and ν_0, α and n are adjustable parameters.

Measurements and laboratory studies suggest a range of values for the adjustable parameters. From a numerical point of view the problem is to determine specific values for these parameters within the context of the numerical model; the optimal parameters selection is the one that simulates the observations best. Ideally, it is necessary to know surface winds and oceanic fields simultaneously for a prolonged period so that the model can be tuned. Although such a data set is unavailable, some progress is possible because certain features of the simulations in which ν and κ have constant values are so poor that improved agreement with observations constitutes a criterion for parameter selection.

There are basically four features in the simulations of *PP* on which we would like to improve:

1) A sharper thermocline. When ν and κ are assigned constant values, those values are usually large and appropriate for the Equatorial Undercurrent where mixing is strong. The models therefore have too much mixing in other regions, especially in and below the thermocline far from the equator. This causes a diffuse thermocline in the models. In reality, the tropical thermocline is very sharp.

2) A more realistic equatorial thermocline. Fig. 1a shows the observed temperature field in the equatorial plane of the Pacific Ocean. Fig. 1b shows this temperature field in the model of *PP*. The simulation is clearly poor.

3) An eastward equatorial jet with little shear in the mixed layer. Eastward winds over the central Indian Ocean in the autumn and spring generate an intense eastward equatorial jet (Knox, 1976; Wyrtki, 1973). This jet is observed to have little vertical shear in the mixed surface layer. In the simulations of *PP* the shear is large.

4) A shoaling of the core of the Equatorial Undercurrent in an eastward direction. The core of the Equatorial Undercurrent is observed to become shallower in an eastward direction, but this does not happen in the models.

Section 2 of this paper briefly describes the model to be used in our studies. Section 3 concerns an appropriate choice for the background mixing parameters ν_b and κ_b in Eqs. (1) and (2). The subjects covered in Sections 4 and 5 are the response of the model to eastward and westward winds respectively, and the sensitivity of these responses to the values of ν and κ. The effect of horizontal mixing is explored in Section 6 where results also are summarized.

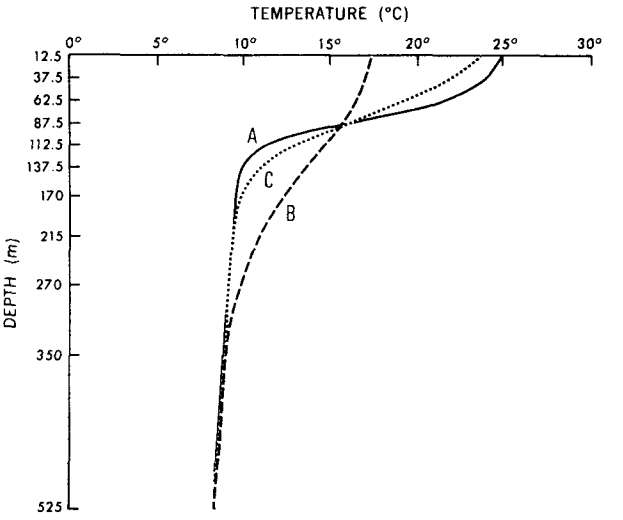

FIG. 2. Profile *A*: The initial temperature field (Below 500 m the temperature decreases linearly to zero.) Profile *B*: The temperature profile after two years because of diffusive spreading associated with $\kappa = 1$ cm^2 s^{-1}. Profile *C*: As in profile *B* but $\kappa = 0.1$ cm^2 s^{-1}.

2. The model

The equations of motion (the primitive equations) are simplified by making the Boussinesq and hydrostatic approximations and by assuming an equation of state of the form $\rho = \rho_0(1 - \alpha T)$ where ρ is the density, T is the temperature, $\alpha = 0.0002°C^{-1}$ is the coefficient of thermal expansion and $\rho_0 = 1$ g cm^{-3}. The coefficients of horizontal eddy viscosity ν_H and thermal diffusivity ν_H are assumed to have the constant values $\nu_H = 2 \times 10^7$ cm^2 s^{-1}, $K_H = 10^7$ cm^2 s^{-1}. The coefficients for vertical eddy mixing are described by equations (1) and (2). The equations are solved numerically by using the method described by Bryan (1969) who discusses the finite-differencing schemes in detail.

The model-ocean is a flat bottom rectangular box with a longitudinal extent of 4800 km, a latitudinal extent of 2800 km (with the equator in the center) and a depth of 3000 m. In a horizontal plane the 70×70 grid points are spaced at regular intervals (of 40 and 70 km in the latitudinal and longitudinal directions, respectively). In the vertical the 16 grid points are spaced irregularly. Fig. 2 shows the distribution of grid points in the upper 525 m.

Motion is forced at the ocean surface by imposing a wind stress. The heat-flux is zero, except in Section 5 where this boundary condition is discussed further:

$$\nu U_z = \tau^x, \quad \nu V_z = 0; \quad w = 0, \quad T_z = 0$$

at $z = 0$ m.

At the vertical walls each of the velocity components and the heat flux are zero.

$$\nu U_z = 0, \quad \nu V_z = 0; \quad T_z = 0 \quad \text{at} \quad z = 3000 \text{ m}.$$

The initial temperature field corresponds to curve *A* in Fig. 2. The model starts from a state of rest. When the winds are eastward, calculations continue for 50 days. For the westward wind stress case, the model is integrated for 300 days to establish equilibrium. (See Philander and Pacanowski, 1980).

3. Diffusive spreading of the thermocline

If κ has a constant value of 1 cm^2 s^{-1} then, even in the absence of any forcing, the initial temperature field (curve *A* in Fig. 2) will change to the field corresponding to curve *B* after 2 years. (This result is obtained by solving the diffusion equation subject to zero flux conditions at the ocean surface and ocean floor.) This considerable diffusive spreading of the thermocline is one of the flaws of the model of *PP*. It can be remedied by assigning κ a value of 0.1 cm^2 s^{-1} in which case *A* in Fig. 2 becomes curve *C* after 2 years. In simulations with the multilevel model and with

$$\nu_b = 1.0 \text{ cm}^2 \text{ s}^{-1}, \quad \kappa_b = 0.1 \text{ cm}^2 \text{ s}^{-1} \qquad (4)$$

for the background mixing, the spreading of the thermocline is indeed very small over a period of a few years. Experiments with much smaller values for these parameters give essentially the same results over a period of 100 days. We therefore adopt the values in Eq (4) for future experiments. The effect of background mixing on other aspects of this solution will be discussed later.

In this section we have considered the appropriate parameter values in regions that are very stable (Ri $\gg$ 1). Next we consider the appropriate values in a mixed layer (Ri $\sim$ 0).

4. Equatorial response to eastward winds

Eastward surface winds drive an intense eastward equatorial jet which is associated with equatorward motion and hence downwelling at the equator. The surface jet is therefore in a mixed layer where vertical temperature gradients are negligible. This is evident in Fig. 3 which shows measurements at the equator when the surface winds are eastward.

We have attempted to simulate the results in Fig. 3 with the model described in Section 2. Of course, simulating all aspects of these results is difficult without knowing the correct initial conditions. We therefore limit our simulation to approximating the shear through the mixed layer. The ocean is initially at rest and the stratification corresponds to curve *A* in Fig. 2. An eastward wind stress of 0.5 dyn cm^{-2} is suddenly imposed. Integrations are continued for 50 days. Experiments were performed for the different values of ν_0, n and α shown in Table 1. In case *A* the coefficients of eddy viscosity and diffusivity have the constant values 10 and 1 cm^2 s^{-1}, respectively.

Fig. 4 shows the dependence of ν on Ri in the different cases listed in Table 1. Fig. 5 shows the vertical structure of the zonal velocity component, on the equator in the middle of the basin, for the different cases listed in Table 1. It is clear that case *A* (which corresponds to constant values for the coefficients of eddy mixing) gives a jet with too large a vertical shear. Results improve when ν and κ are variable. An increase in the value of ν_0 decreases the speed and shear of the jet. Variations in α and n alter the speed but not the shear.

The temperature on the equator in the center of the basin is almost the same for all the different cases in Table 1. Fig. 6 shows the temperature profiles corresponding to cases *A* and *D*.

On the basis of these results any of the parameter values corresponding to cases *C* through *G* are acceptable. We therefore propose

$$50 \leq \nu_0 \leq 150 \text{ cm}^2 \text{ s}^{-1}. \qquad (5)$$

This range is sufficiently wide to make it unnecessary for α and n to vary too. In future experiments we therefore assign n and α the values

$$n = 2, \quad \alpha = 5. \qquad (6)$$

If background values for vertical mixing of heat and momentum are reduced by two orders of magnitude (to essentially molecular values) results do not change substantially.

5. The equatorial response to westward winds

Eastward winds cause surface waters to converge on the equator where there is downwelling and a mixed surface layer. Simulation of this mixing in the upper ocean does not pose a serious problem (see Section 4). Westward winds cause equatorial upwelling of cold water; this counters the downward mixing of warm water. We expect it to be more difficult to strike the right balance between these opposing processes. Fig. 1 shows that the results are unsatisfactory when ν and κ have constant values of 10 and 1 cm^2 s^{-1}m, respectively. There apparently is too little mixing because the model has no mixed layer at all. Fig. 7 shows the results for variables ν and κ with

$$\left.\begin{aligned} \nu_0 &= 100 \text{ cm}^2 \text{ s}^{-1}, \quad n = 2, \quad \alpha = 5 \\ \nu_b &= 1 \text{ cm}^2 \text{ s}^{-1}, \quad \kappa_b = 0.1 \text{ cm}^2 \text{ s}^{-1} \end{aligned}\right\}.$$

The vertical spreading of the thermocline has been inhibited, and there is a mixed surface layer. How-

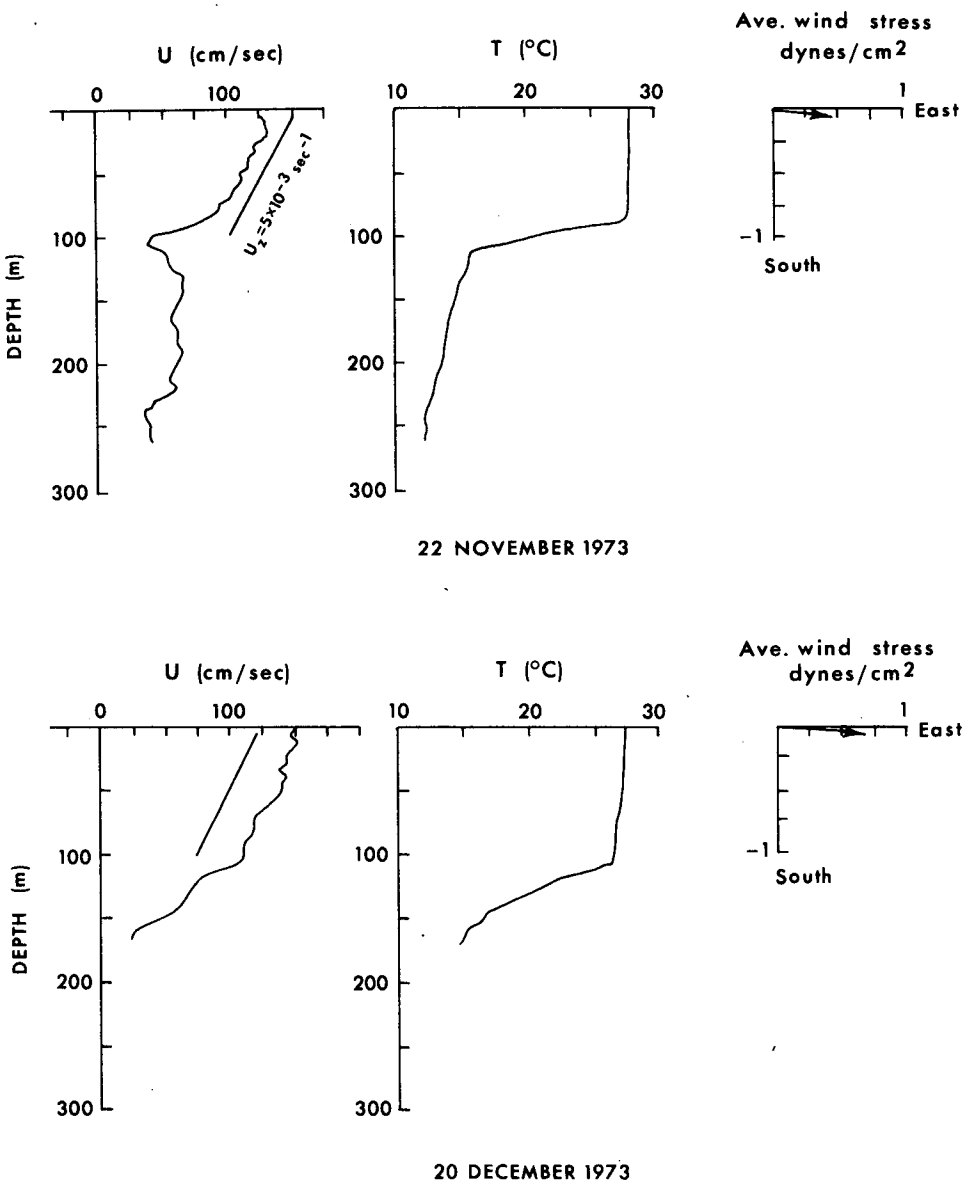

FIG. 3. Zonal velocity and temperature measurements on the equator near Gan (70°E) at a time when the eastward wind stress was 0.5 dyn cm^2. After Knox and McPhaden (1976).

ever, the depth of the mixed layer does not vary from west to east—so that the thermocline has no zonal slope—and the maximum speed of the Equatorial Undercurrent is only 30 cm s^{-1}. (Measurements suggest that it should be twice as intense for the imposed windstress of -0.5 dyncm^{-2}). These flaws indicate that there is too much mixing. An experiment in which $\nu_0 = 20$ cm^2 s^{-1} gives a speedier Undercurrent but the mixed layer has no east–west slope. Furthermore, this value for ν_0 gives poor results when the winds are eastward (see Section 4).

In all the experiments described so far a condition of no heat flux has been imposed at the surface. This is justifiable for regions with a mixed surface layer but is inappropriate for the eastern Pacific where there is no mixed layer and where the sea surface temperature is less than the air temperature. (See Fig. 1). A positive heat flux into the ocean will stabilize the upper layers and hence decrease mixing processes there. This effect could be considerable because the values of ν and κ are very sensitive to the value of the Richardson number Ri at small values of Ri (see Fig. 4). To investigate this possible effect associated with a nonzero surface

TABLE 1. Parameter choices for the eastward wind stress case.

Case	ν_0 (cm^2 s^{-1})	n	α
A	—	—	—
B	20	2	5
C	50	2	5
D	100	2	5
E	100	1	5
F	150	2	5
G	150	2	10

heat flux we adopt Haney's (1971) parameterization of the heat exchange between the ocean and atmosphere:

$$\kappa T_z = \gamma(-T + T^*). \quad (7)$$

The constant γ is approximately 70 ly °C^{-1} day for equatorial regions. T is the temperature of the ocean at the surface and T^* is the temperature of the atmosphere.

We repeated the experiment $\nu_0 = 50$ cm^2 s^{-1}, $n = 2$, $\alpha = 5$ but with the boundary condition (7) and $T^* = 25$°C. The results are now very realistic. Furthermore, they are relatively insensitive to changes in the value of ν_0: an experiment in which ν_0 is decreased from 100 to 50 cm s^{-2} gives essentially the same temperature field, and gives an Undercurrent with a maximum speed that is only 15% higher. Results for the latter experiment are shown in Fig. 8.

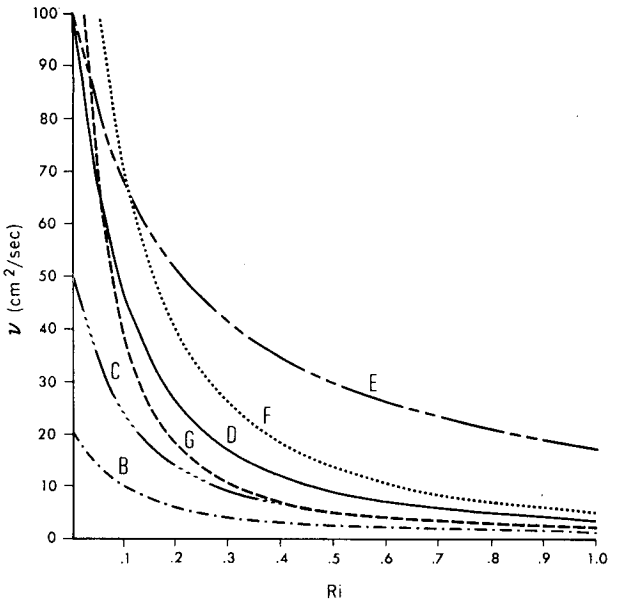

FIG. 4. The dependence of ν on Ri for the different cases listed in Table 1.

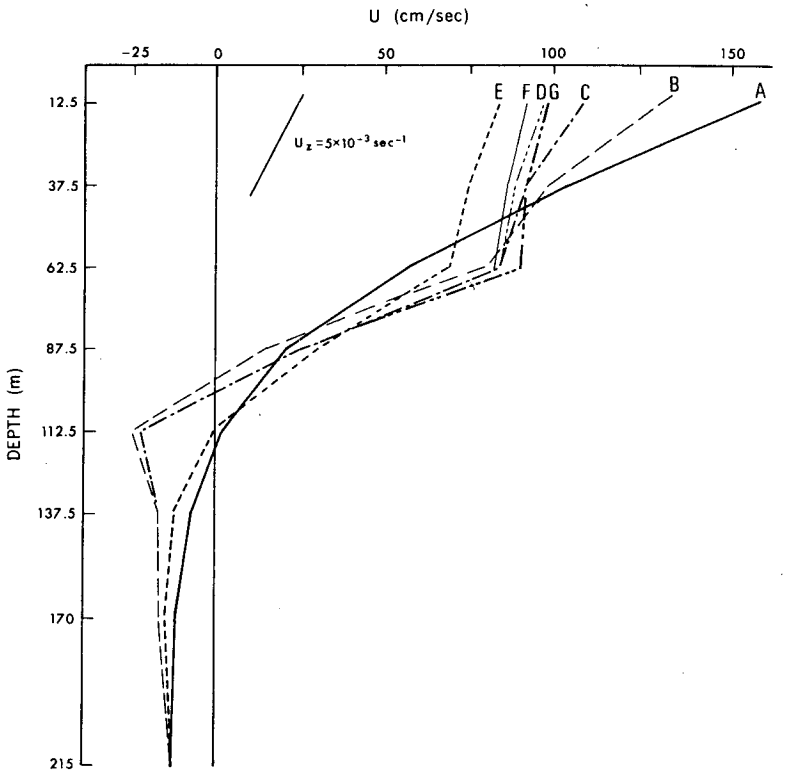

FIG. 5. The vertical structure of the zonal velocity component on the equator in the center of the basin in response to eastward winds of intensity 0.5 dyn cm^{-2}, for the different cases listed in Table 1.

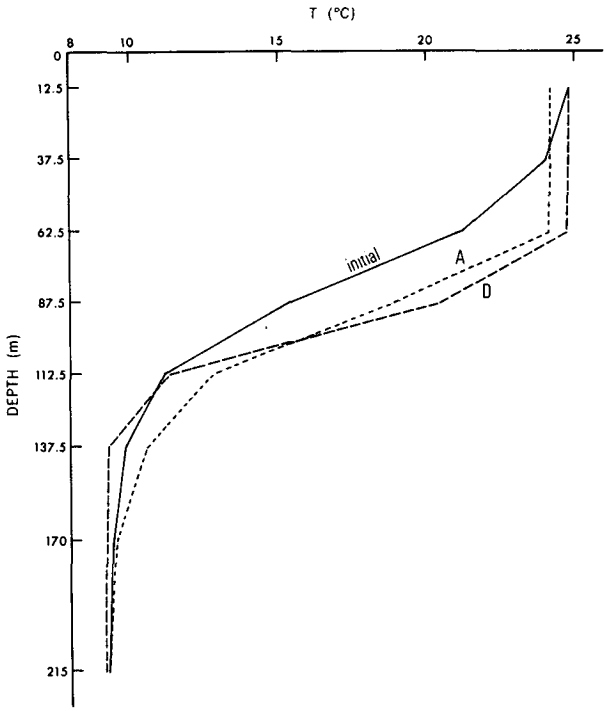

FIG. 6. The vertical structure of the temperature field associated with the zonal velocity component in Fig. 4a, for cases *A* and *D* in Table 1.

The principal result so far is that the heat flux condition at the ocean surface significantly affects mixing processes there. This, in turn, affects the character of the flow. A realistic surface boundary condition results in realistic simulations which are

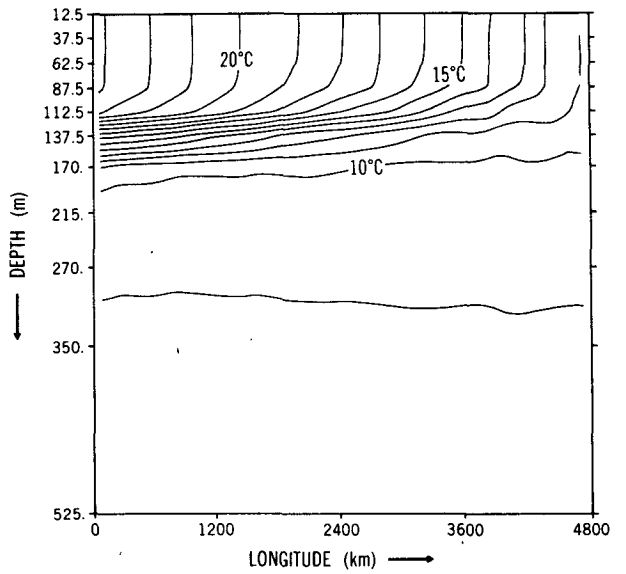

FIG. 7. Temperatures in the equatorial plane when the surface heat flux is zero and $\nu_0 = 100$ cm^2 s^{-1}.

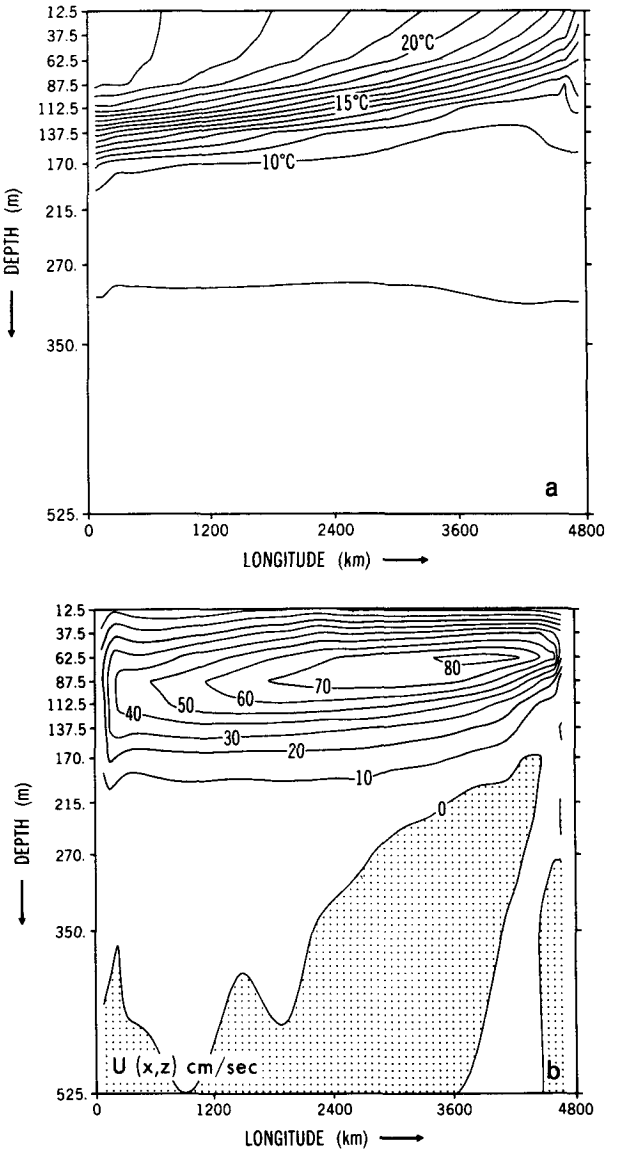

FIG. 8. (a) Temperature and (b) Zonal velocity component in the equatorial plane when there is surface heat flux according to Eq. (7) and $\nu_0 = 50$ cm^2 s^{-1}.

insensitive to the specific value of ν_0 provided it is O (50 cm^2 s^{-1}).

Fig. 9 shows the value of ln Ri for the motion depicted in Fig. 8. Note that mixing is intense in the surface layers and in the "thermostad" below the core of the Equatorial Undercurrent (where Ri has a maximum). The simulated thermostad is unrealistic in two respects: mixing is not sufficiently intense there; in the model the thermostad is confined to a region immediately below the core of the Undercurrent whereas it has a considerable latitudinal extent (to about 5°N and *S*) in reality. Smaller background values for vertical mixing of heat and momentum result in a more realistic thermostad

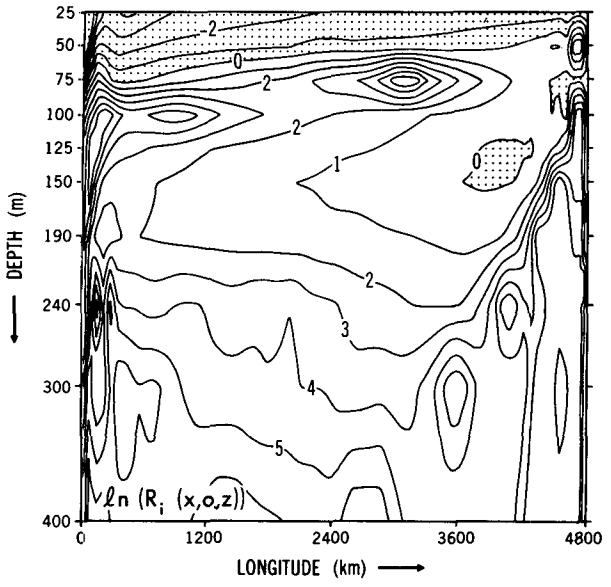

FIG. 9. The value of ln Ri (negative values are shaded) in the equatorial plane for the conditions shown in Fig. 8.

because it causes the shear of the Undercurrent, and hence the intensity of the mixing, to increase (cf. Figs. 10a and 10b).

6. Conclusion

The parameterization for mixing described by Eqs. (1) and (2) gives much better results than constant values for ν and κ provided

$$\nu_b = 1 \text{ cm}^2 \text{ s}^{-1},$$
$$\kappa_b = 0.1 \text{ cm}^2 \text{ s}^{-1},$$
$$n = 2,$$
$$\alpha = 5,$$
$$\nu_0 = \text{O}\,(50 \text{ cm}^2 \text{ s}^{-1}).$$

It is important that appropriate heat flux conditions at the ocean surface be specified because these conditions affect the stability of the upper ocean, and hence the intensity of mixing there. With the appropriate surface boundary condition the results are relatively insensitive to the value of ν_0 (which is the value of ν under neutral conditions Ri = 0).

In addition to the parameterization scheme of Eqs. (1) and (2), we also made calculations that use the turbulent closure scheme of Mellor and Durbin (1975). In this scheme there are no adjustable parameters (except for the choice of background mixing) since all constants are determined from neutral turbulent flow data. We found that the coefficients ν and κ either have values that are practically zero, or at very low Richardson numbers, have values that are O (1000 cm^2 s^{-1}). Such high values result in computational difficulties that can be overcome by limiting the maximum values of ν and κ, and by decreasing the time step of the numerical integrations. The results obtained are similar to those described earlier but from a computational point of view the method is less efficient than the parameterization of Eqs. (1) and (2).

In the calculations described so far we have assumed the constant values 2 × 10^7 and 1 × 10^7 cm^2

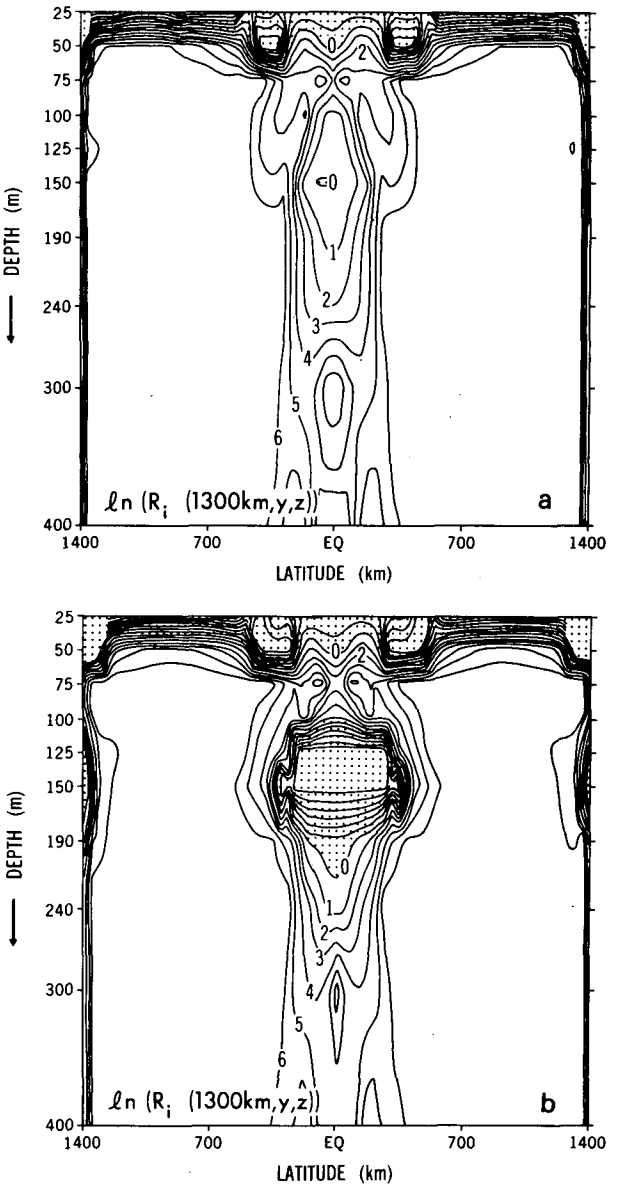

FIG. 10. (a) The value of ln Ri (negative values are shaded) in a meridional plane 1300 km from the eastern boundary for the conditions shown in Fig. 8. (b) As Fig. 10a except background values for vertical mixing of heat and momentum have been reduced by two orders of magnitude.

s^{-1} for the coefficients that parameterize the horizontal mixing of momentum and heat respectively. On the basis of measurements in the core of the Undercurrent in the Atlantic, Katz *et al.* (1979) estimate a value of 2×10^7 cm^2 s^{-1} for the latitudinal mixing of salt. There are no indications as to how this value varies with space or time. It is noteworthy that the results of the model are sensitive to changes in the values assigned to these coefficients. A reduction from 2×10^7 to 1×10^7 cm^2 s^{-1} in the coefficient for the horizontal mixing of momentum, increases the maximum speed of the Undercurrent from 80 to 105 cm s^{-1}, increases the shear of this current and thus enhances mixing in the thermostad. The measurements of Katz *et al.* (1979) suggest a value of the order of 10^7 cm^2 s^{-1} but at this stage there is no reason to believe that a value of 1×10^7 cm^2 s^{-1} is more appropriate than a value that is somewhat smaller or larger. We do not know whether the intensity of the Undercurrent should be 80 cm s^{-1} or 100 cm s^{-1} in response to steady 0.5 dyn cm^2 winds because such winds do not prevail anywhere. What we need are time series that describe how the currents and density field vary when the winds vary on long time scales. Attempts to simulate such a data set will suggest the appropriate value for mixing coefficients.

To improve on the parameterization of vertical mixing we need further measurements of mixing rates under different large-scale conditions. The intensity of the Equatorial Undercurrent (and hence its vertial shear) varies with time (seasonally and interannually) and with position. (The Undercurrent is much more intense in the central Pacific than in the eastern Pacific or Atlantic Oceans.) It should therefore be possible to determine whether the Richardson number dependence in Eqs. (1) and (2) is accurate.

Acknowledgments. We wish to thank Betty Williams for typing and Phil Tunison for drafting the figures for this manuscript.

REFERENCES

Bryan, K., 1960: A numerical method for the study of the world ocean. *J. Comput. Phys.*, **4**, 347–376.

Colin, C., C. Henin, P. Hisard and C. Oudot, 1971: Le Courant de Cromwell dans le Pacifique central en février. *Cah. ORSTOM Ser. Oceanogr.*, **7**, 167–186.

Crawford, W. R., and T. R. Osborn, 1979a: Microstructure measurements in the Atlantic Equatorial Undercurrent during GATE. *Deep-Sea Res.*, **26**(Supp. II), 285–308.

——, and ——, 1979b: Energetics of the Atlantic Equatorial Currents. *Deep-Sea Res.*, **26**(Supp. II), 309–324.

Gregg, M. C., 1976: Temperature and salinity microstructure of the Pacific Equatorial Undercurrent. *J. Geophys. Res.*, **81**, 1180–1196.

Halpern, D., 1980: Variability of near-surface currents in the Atlantic North Equatorial Countercurrent during GATE. *J. Phys. Oceanogr.*, **10**, 1213–1220.

Haney, R. H., 1971: Surface thermal boundary conditions for ocean circulation models. *J. Phys. Oceanogr.*, **1**, 241–248.

Hughes, R. L., 1980: On the equatorial mixed layer. *Deep-Sea Res.*, **27**, 1067–1078.

Jones, J. H., 1973: Vertical mixing in the Equatorial Undercurrent. *J. Phys. Oceanogr.*, **3**, 286–296.

Katz, E. J., J. G. Bruce and B. D. Petrie, 1979: Salt and mass flux in the Atlantic Equatorial Undercurrent. *Deep-Sea Res.*, **26**(Supp. II), 137–160.

Knox, R., 1976: On a long series of measurements of Indian Ocean equatorial currents near Addu Atoll. *Deep-Sea Res.*, **23**, 211–221.

——, and M. J. McPhaden, 1976: Profiles of velocity and temperatures near the Indian Ocean equator. Scripps Inst. Oceanography, SIO Ref. Series 76.11, 96 pp.

Kraus, E. B., and J. S. Turner, 1967: A one-dimensional model of the seasonal thermocline. *Tellus*, **19**, 98–106.

Mellor, G. L., and P. A. Durbin, 1975: The structure dynamics of the ocean surface mixed layer. *J. Phys. Oceanogr.*, **5**, 718–728.

Osborn, T. R., and L. E. Bolodean, 1980: Temperature microstructure in the Atlantic Equatorial Undercurrent. *J. Phys. Oceanogr.*, **10**, 66–82.

Philander, S. G. H., and R. C. Pacanowski, 1980: The generation of equatorial currents. *J. Geophys. Res.*, **85**, 1123–1136.

——, and ——, 1981: The response of equatorial oceans to periodic forcing. *J. Geophys. Res.*, **86**, 1903–1916.

Robinson, A. R., 1966: An investigation into the wind as the cause of the Equatorial Undercurrent. *J. Mar. Res.*, **24**, 179–204.

Semtner, A. J., and W. R. Holland, 1980: Numerical simulation of equatorial ocean circulation. *J. Phys. Oceanogr.*, **10**, 667–693.

Wyrtki, K., 1973: An equatorial jet in the Indian Ocean. *Science*, **181**, 262–264.